



Contents lists available at ScienceDirect

Journal of Human Evolution

journal homepage: www.elsevier.com/locate/jhevol

Patterns of lateral enamel growth in *Homo naledi* as assessed through perikymata distribution and number

Debbie Guatelli-Steinberg^{a, b, *}, Mackie C. O'Hara^a, Adeline Le Cabec^c,
Lucas K. Delezene^{d, e}, Donald J. Reid^f, Matthew M. Skinner^{b, c, e}, Lee R. Berger^e

^a Department of Anthropology, The Ohio State University, Columbus, OH, USA

^b School of Anthropology and Conservation, University of Kent, Canterbury, UK

^c Department of Human Evolution, Max Planck Institute for Evolutionary Anthropology, Leipzig, Germany

^d Department of Anthropology, University of Arkansas, Fayetteville, AR, USA

^e Evolutionary Studies Institute and the National Centre for Excellence in Palaeosciences, University of the Witwatersrand, Wits, South Africa

^f Department of Anthropology, The George Washington University, Washington D.C., USA

ARTICLE INFO

Article history:

Received 25 October 2017

Accepted 21 March 2018

Available online xxx

Keywords:

Dental development

Hominin teeth

Fossil teeth

Rising Star Cave

Dinaledi Chamber

ABSTRACT

Perikymata, incremental growth lines visible on tooth enamel surfaces, differ in their distribution and number among hominin species, although with overlapping patterns. This study asks: (1) How does the distribution of perikymata along the lateral enamel surface of *Homo naledi* anterior teeth compare to that of other hominins? (2) When both perikymata distribution and number are analyzed together, how distinct is *H. naledi* from other hominins? A total of 19 permanent anterior teeth (incisors and canines) of *H. naledi* were compared, by tooth type, to permanent anterior teeth of other hominins: *Australopithecus afarensis*, *Australopithecus africanus*, *Paranthropus robustus*, *Paranthropus boisei*, *Homo ergaster*/*Homo erectus*, other early *Homo*, Neandertals, and modern humans, with varying sample sizes. Repeated measures analyses of the percentage of perikymata per decile of reconstructed crown height yielded several statistically significant differences between *H. naledi* and other hominins. Canonical variates analysis of percentage of perikymata in the cervical half of the crown together with perikymata number revealed that, in 8 of 19 cases, *H. naledi* teeth were significantly unlikely to be classified as other hominins, while exhibiting least difference from modern humans (especially southern Africans). In a cross-validated analysis, 68% of the *H. naledi* teeth were classified as such, while 32% were classified as modern human (most often southern African). Of 313 comparative teeth used for this analysis, only 1.9% were classified as *H. naledi*. What tends to differentiate *H. naledi* anterior tooth crowns from those of most other hominins, including some modern humans, is strongly skewed perikymata distributions combined with perikymata numbers that fall in the middle to lower ranges of hominin values. *H. naledi* therefore tends toward a particular combination of these features that is less often seen in other hominins. Implications of these data for the growth and development of *H. naledi* anterior teeth are considered.

© 2018 Elsevier Ltd. All rights reserved.

1. Introduction

In the original description of the Dinaledi fossils, Berger et al. (2015) concluded that the skeletal and dental features of these small-brained and small-bodied hominins allowed their inclusion within the genus *Homo*, but were distinct enough to warrant a new species: *Homo naledi*. Paleoanthropologists generally accepted the

first conclusion but, initially, some questioned the second (Randolph-Quinney, 2015). Ensuing analyses supported the inclusion of the Dinaledi fossils into the genus *Homo*, as well as its distinctiveness as a species (Thackeray, 2015; Dembo et al., 2016; Garvin et al., 2017), but differed with respect to its affinities to other *Homo* species. Comparative analyses of dental morphology (e.g., Berthaume et al., in press; Irish et al., in review; Bailey et al., in review) have supported the conclusion that *H. naledi* is distinct from all other hominins and is best placed within the genus *Homo*. A recent study indicated that the remains of *H. naledi* from the Dinaledi Chamber were deposited between 236 and 335 ka (Dirks

* Corresponding author.

E-mail address: guatelli-steinbe.1@osu.edu (D. Guatelli-Steinberg).

et al., 2017). Additional fossils of *H. naledi* have recently been found nearby in the Lesedi Chamber (Hawks et al., 2017), but are not yet dated.

The rich dental sample of *H. naledi* (Berger et al., 2015; Hawks et al., 2017) provides an opportunity not only for further analysis of the species' morphometric affinities, but also of its dental growth and development. The present contribution addresses aspects of dental enamel growth in *H. naledi* from the non-destructive analysis of perikymata, growth increments on the enamel surface that are continuous with underlying striae of Retzius. The latter are dark lines visible in enamel ground sections that represent a rhythmic slowing in enamel matrix secretion (Hillson, 2014). In the lateral enamel of teeth (i.e., not at cusp tips), each stria of Retzius is continuous with a single perikyma, such that both structures form in response to the same growth rhythm (Fig. 1). The periodicity of this rhythm is constant within the permanent teeth of each individual (FitzGerald, 1998), ranging from 6 to 12 days in modern humans (Reid and Dean, 2006), with some studies reporting rare values of 5 days (Kawasaki et al., 1977; Dean et al., 1993; Huda and Bowman, 1994). In earlier hominins, periodicities extend from 5 days at the low end of this spectrum to 13 days on the high end (Smith et al., 2015).

The present study analyzes how perikymata are distributed on the enamel surfaces of *H. naledi* and how their distribution compares to that of other hominins. Perikymata distribution appears to differ among hominin species (though with overlap among species), likely reflecting differences in their patterns of enamel growth (Dean and Reid, 2001a; Guatelli-Steinberg et al., 2007, 2016; Xing et al., 2015). In modern humans, the distribution of perikymata in the lateral enamel of teeth is related to changes in rates of enamel extension from cusp to cervix (Guatelli-Steinberg et al., 2012). Enamel extension rates are the rates at which crowns grow in height (Dean, 2009). More specifically, they are the rates at which ameloblasts (enamel-forming cells) differentiate from the inner enamel epithelium along what will

become the enamel-dentine junction (EDJ) in the mature crown (Shellis, 1984).

Modern humans (specifically, northern Europeans and southern Africans) exhibit both a decrease in rates of enamel extension as lateral enamel formation proceeds and an associated decrease in the spacing of perikymata (Guatelli-Steinberg et al., 2012). Furthermore, per decile of crown height, individuals with steeper declines in enamel extension rates tend to also have steeper declines in perikymata spacing. These findings demonstrate a relationship between the rates of enamel extension and distribution of perikymata on the crown surface in modern humans. Despite these findings, it is currently unknown if this relationship holds among hominin species, because a comparative study of the various factors that can affect perikymata distribution has yet to be undertaken across extinct species. Such factors include not only rates of enamel extension, but also the daily rate of enamel matrix secretion near both the EDJ (Shellis, 1984) and the outer enamel surface (Dean and Shellis, 1998), as well as the surface contour of a tooth (Hillson and Bond, 1997). Consequently, it is important to bear in mind that perikymata distribution differences across hominin species suggest enamel growth pattern differences, but the exact growth processes underlying them are unknown.

Dean and Reid (2001a) published the first comparative analysis of perikymata distribution in hominin anterior teeth. They plotted the number of days of estimated enamel formation time (using perikymata counts and estimated periodicities) per decile of crown height for various hominin species, with deciles numbered from the cusp tip (first decile) to the cervix (tenth decile; Fig. 2). For modern humans, the number of days to form each decile increased steeply at the start of the third decile, but then decreased in the last decile. With the exception of OH 7, the type specimen of *Homo habilis*, all other hominins were marked by more gradually increasing growth curves beginning at decile 3 and did not exhibit the same drop in the last decile. The most gradual growth curves, reflecting more evenly spaced perikymata along the deciles of

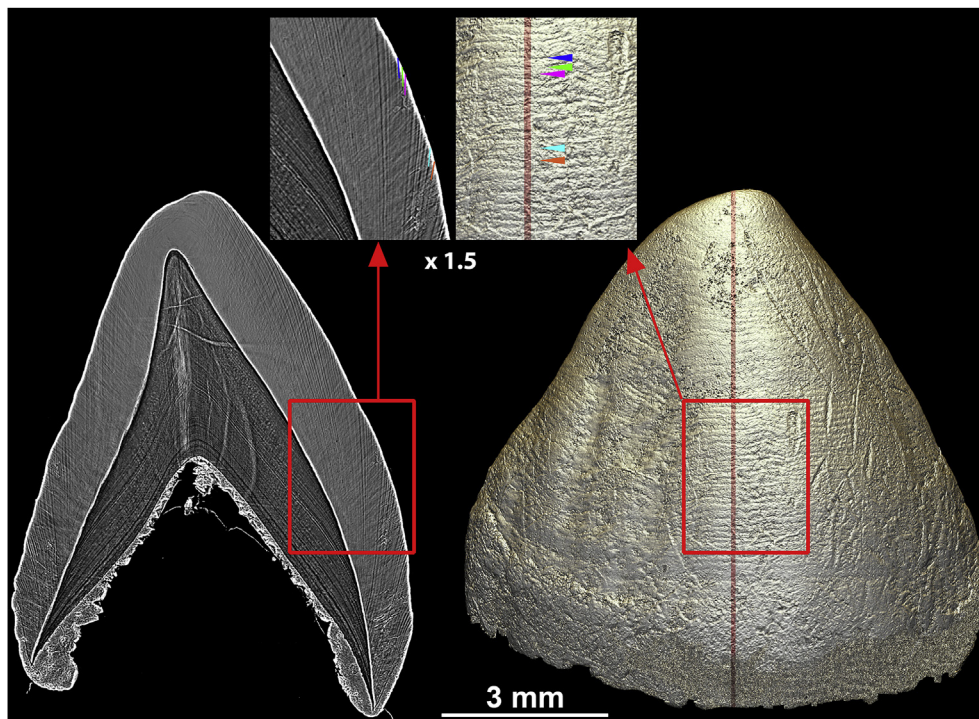


Figure 1. Virtual 2D section and 3D model of the enamel cap of the STS2 upper left canine (modified after Le Cabec et al., 2015:Fig. 9) showing the matching between the incremental growth lines in the enamel—Retzius lines—on the 2D section, with their manifestation on outer enamel surface as perikymata on the 3D model.

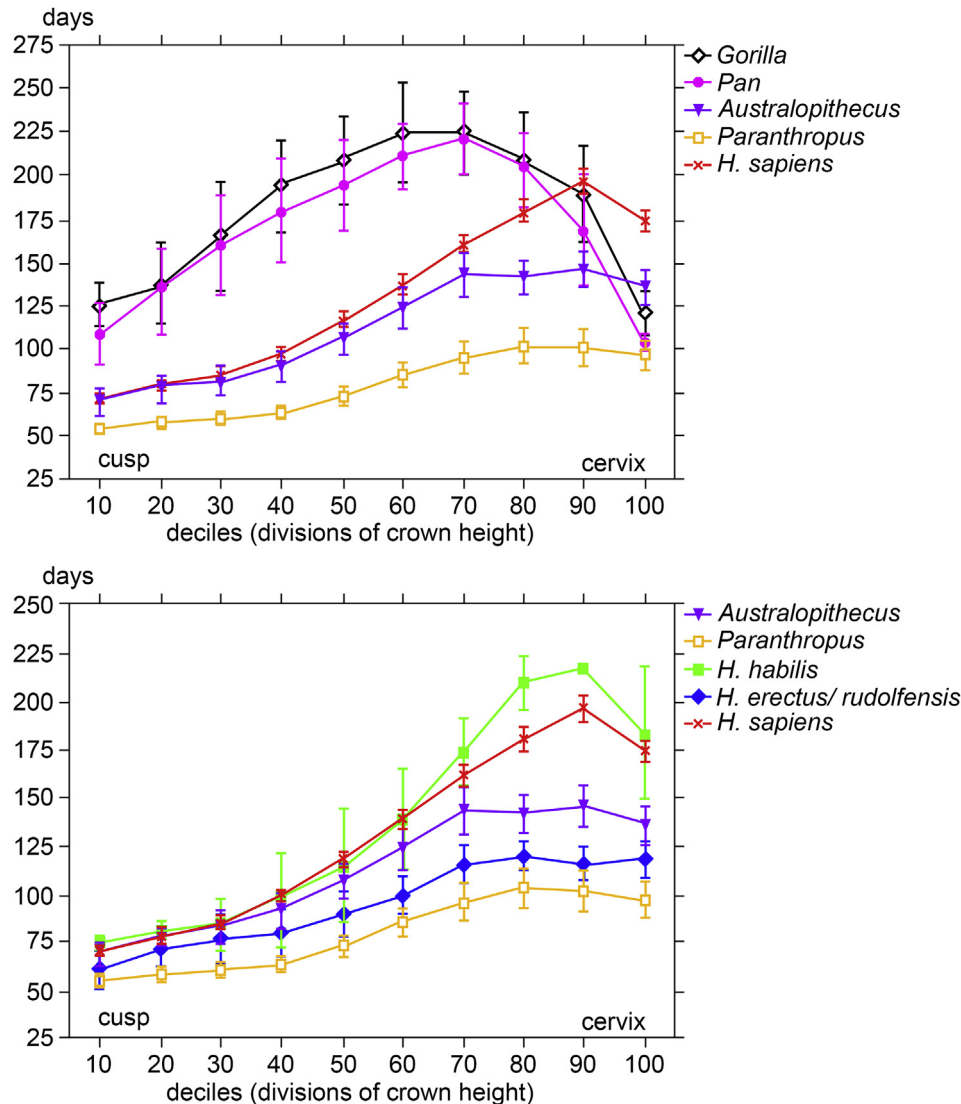


Figure 2. The distribution of the number of days of growth per decile in hominoids (upper plot) and hominins (lower plot). Deciles are numbered from 1 (cusp tip) to 10 (cervix). The number of days was calculated by multiplying the number of perikymata in each decile by the species' average periodicity. Error bars represent the 95% confidence limits of the mean. These graphs are from [Dean and Reid \(2001a:Fig. 2\)](#) and are published here with permission from John Wiley and Sons (License number 4037780016882, Jan. 28, 2017).

crown height, were found in *Paranthropus* and in the pooled sample of *Homo erectus* and *Homo rudolfensis*. *Australopithecus* growth curves appeared to increase in steepness more rapidly than those of these taxa, but less rapidly than those of modern humans, and again did not exhibit the decline in decile 10 that modern humans do.

To generalize, the most common pattern [Dean and Reid \(2001a\)](#) found in extinct hominins was that the number of perikymata per decile of crown height does not increase to the same extent as it does in modern humans. For each anterior tooth type, modern humans generally exhibit both a greater number of perikymata ([Dean et al., 2001](#)) and a perikymata distribution pattern in which their additional perikymata are packed preferentially into later deciles of the crown. Subsequent studies found that, although Neandertals do not appear to have more perikymata per tooth type than do modern humans ([Guatelli-Steinberg et al., 2005, 2007](#)), they have a more gradual increase in perikymata across their deciles of crown height than do modern humans ([Ramirez-Rozzi and Bermúdez de Castro, 2004; Guatelli-Steinberg et al., 2007](#)). [Modesto-Mata et al., 2014](#) showed that the Sima de los Huesos

hominins (dated to 430 ka; [Arsuaga et al., 2014](#)) were similar to Neandertals in this regard.

Thus, although there are exceptions to be found in OH 7 ([Dean and Reid, 2001a](#)), and possibly also in the teeth of some other early *Homo* ([Guatelli-Steinberg et al., 2016](#)), a more uniform distribution of perikymata is usually found in earlier hominins, even when the number of perikymata on their teeth is equivalent to that of modern humans ([Xing et al., 2015; Guatelli-Steinberg et al., 2016](#)). The latter finding suggests that perikymata distribution and perikymata number can be dissociated (i.e., equivalence in perikymata number does not imply equivalence in perikymata distribution pattern) and that different hominin species may have different combinations of the two ([Xing et al., 2015; Guatelli-Steinberg et al., 2016](#)).

The present study asks where *H. naledi* falls with respect to other hominins in its patterns of enamel growth. Does it exhibit a more uniform distribution of perikymata like most earlier hominins or does it exhibit a steeper increase in perikymata similar to that of modern humans? Furthermore, how does enamel growth compare to various species when both perikymata distribution and

perikymata number are considered simultaneously? The present study represents a first step in characterizing the lateral enamel growth patterns of this species.

2. Materials and methods

2.1. Dental sample and perikymata counting

The maximum number and type of permanent anterior teeth (incisors and canines) included in this study are given by taxon in [Table 1](#): *H. naledi* ($n = 19$), and the comparative sample (total $n = 328$), comprising a pooled sample of *Australopithecus afarensis* and *Australopithecus africanus*, *Paranthropus robustus*, *Paranthropus boisei*, *Homo ergaster*/*H. erectus*, early *Homo* (*H. habilis*/*H. rudolfensis*), Neandertals (i.e., *Homo neanderthalensis*)¹ and *Homo sapiens* (specifically, recent modern humans, including: Inupiaq, northern Europeans from Newcastle-Upon-Tyne, and southern Africans). Note that different sets of analyses were performed on different subsamples, and these are reported along with the analyses to which they pertain.

Samples were divided in the following manner: (1) *Australopithecus* samples were combined because of small sample sizes; (2) *Paranthropus* samples were separated, owing to previous analyses suggesting differences in their perikymata distribution ([Dean, 1987](#)); (3) *H. ergaster*/*H. erectus* was separated from other early *Homo* (i.e., *H. habilis*, *H. rudolfensis*) in order to directly compare *H. naledi* to *H. ergaster*/*H. erectus* (a taxon to which some have argued it may belong; see [Randolph-Quinney, 2015](#)). For this study, only *H. naledi* teeth from the Dinaledi chamber, site U.W. 101 ([Berger et al., 2015](#)), were considered, as the few anterior teeth from the Lesedi chamber, site U.W. 102 ([Hawks et al., 2017](#)), were either too worn or lacked enamel near the cervix because their crowns were not completely formed. For the comparative samples, the following data sources were used: *Australopithecus* and *Paranthropus* data are from [Dean and Reid \(2001b\)](#); early *Homo* and *H. ergaster*/*H. erectus* data were shared by Christopher Dean and Donald Reid, included in the *Homo* samples of [Dean et al. \(2001\)](#) and [Dean and Reid \(2001a\)](#), and published in [Xing et al. \(2015\)](#) and [Guatelli-Steinberg et al. \(2016\)](#); and Neandertal and modern human data are from [Guatelli-Steinberg et al. \(2005, 2007\)](#). It is important to note that the early *Homo* and *H. ergaster*/*H. erectus* sample sizes are small and include teeth from some individuals (e.g., KNM-ER 1590 and KNM-ER 820) on which perikymata are not as clear as they are on others (e.g., OH 7 and KNM-WT 15000). No lower canine teeth were included in this study, as the enamel surface on *H. naledi* lower canines was often uneven, making it difficult to clearly distinguish perikymata from one another.

For the *H. naledi* sample, high-resolution impressions of labial surfaces were made (by D.G.S. and Mark F. Skinner) with President's Jet Regular Body and cast (by D.G.S. and M.C.O.) in Struers' Epofix, a high-resolution epoxy. Prior to casting, microcomputed tomography (μ CT) images of the fragile teeth of *H. naledi* were screened for enamel cracks (by A.L.C. and M.C.O.), such that only those teeth without enamel cracks running from the EDJ to the outer enamel surface were used (O'Hara et al., in prep.). For the comparative samples, similar casting methods were used for *Australopithecus*, *Paranthropus*, early *Homo* ([Dean and Reid, 2001a](#)), Neandertals and

Inupiaq ([Guatelli-Steinberg et al., 2005, 2007](#)). Histological samples were used for the southern African and Newcastle teeth ([Reid and Dean, 2006](#)).

Only teeth estimated to have 80% of their crown heights intact were retained for analysis in this study. If both anteriors were present, the tooth with less occlusal wear was chosen. For the comparative samples, these estimates were made by eye, by comparing the morphology of worn teeth to that of unworn or minimally worn teeth (and for the histological samples, by visually extending the sides of the tooth sections). For the sample of *H. naledi*, a more precise method was used following that of [Saunders et al. \(2007\)](#) and originally designed for use in histological canine sections. (A recent study has also focused on reconstructing worn crowns, though in human molars; [Modesto-Mata et al., 2017](#).) In the [Saunders et al. \(2007\)](#) method, tangent lines are drawn with the line tool in Adobe Photoshop® on either side of the crown. Then the pen tool is used to reconstruct the missing cusp tip of the crown by extending lines drawn tangent to the sloping sides of the crown and automatically filling in a rounded cusp between the extended lines.

The same procedure was used here (by M.C.O. using Adobe Photoshop® CC Version 2017.0.1) on 2D μ CT slices of *H. naledi* teeth taken through the sharpest point of the dentine horn, essentially creating a digitally rendered sagittal section, like those used by [Saunders et al. \(2007\)](#). The method can be directly applied here because μ CT cross sections of incisor have sloping sides that can be extended along a tangent to meet at the apex, just as a canine does. The reconstructed crown height was then measured in ImageJ 1.50e ([Rasband, 2016](#)) and compared to the crown height of the cast to obtain the percentage of crown height present ([Fig. 3](#)). Additional detail and validation of this reconstruction method using μ CT data also for incisors is discussed in O'Hara et al. (in prep.), in which the average error was calculated by digitally removing cuspal portions of complete crowns and then reconstructing them with the [Saunders et al. \(2007\)](#) method. The average error across tooth types was 0.30%, with upper canines showing the greatest error at 1.21%. The errors were not systematic: they were equally likely to under- as to overestimate the crown height. The fact that the error is small can largely be attributed to these causes: (1) consistency in how the lines tangent to the crown surface are drawn, (2) the fact that Adobe Photoshop® completes the missing portion according to where the tangent lines are drawn, and (3) the fact that the portion that is reconstructed (the cusp tip) represents only a small portion of the overall crown height. For the purpose of further documentation, we also include wear scores for the *H. naledi* sample based on the method of [Smith \(1984\)](#) in Supplementary Online Material (SOM Table S1).

Perikymata were counted in deciles of reconstructed crown height. In the comparative replica samples, perikymata were counted under a light microscope, with replicas oriented perpendicularly to the microscope's optical axis ([Dean and Reid, 2001a](#); [Guatelli-Steinberg et al., 2007](#)). Transmitted light microscopy was used for the histological samples. Perikymata were counted in these samples by counting striae of Retzius close to the outer enamel surface, where they emerge as perikymata, thus ensuring comparability between data derived from tooth replicas and histological samples ([Guatelli-Steinberg et al., 2005, 2007](#); [Reid and Dean, 2006](#)). For the sample of *H. naledi*, perikymata were counted by clicking on each perikyma under a measuring microscope (Olympus U-CMAD 3 with VisionGauge 1.0 software), recording the X, Y, and Z coordinates of each perikyma. In deciles of the crown where perikymata were difficult to discern under the measuring microscope (which has a shallow depth of field), counts were made under a Leica DMS 1000 digital monocular microscope. Magnifications ranged from 15 \times to 50 \times , depending on the density of

¹ Although Neandertals are customarily considered a distinct species (*Homo neanderthalensis*) from modern humans (*Homo sapiens*; see [Harvati et al., 2004](#)), some authors argue that the former may be a subspecies of the latter and that the taxonomic position of Neandertals therefore remains unresolved (e.g., [Ahern et al., 2005](#)). Here, we follow [Reich et al. \(2010:1059\)](#), in using the term "Neandertals" in order to "refrain from any formal Linnaean taxonomic designations that would indicate species or subspecies status".

Table 1
Sample of *Homo naledi* and comparative taxa used in this study.

	I_1	I_2	I^1	I^2	C^1
<i>Australopithecus spp.</i> ^a (N = 17)	n = 3 (LH 2, Sts 24, Sts 52a/b)	n = 1 (StW 425)	n = 5 (LH 3, MLD 43, Sts 24a, Sts 52 a/b, StW 183)	n = 5 (LH 3, LH 6, MLD 11, Sts 52a/b, Sts 24a)	n = 3 (MLD 11, Sts 52a/b, StW 183)
<i>Paranthropus boisei</i> (N = 5)	n = 4 (KNM-ER 812, KNM-ER 1477, KNM-ER 1820, OH 30)	n = 1 (KNMER 3230)	—	—	—
<i>Paranthropus robustus</i> (N = 21)	n = 4 (SKX 5004b, SK 62, SK 63, SK 852)	n = 2 (SK 63, KB 5223)	n = 7 (SK 68, SK 69, SK 73, SKX 240, SKX 271, SKX 3300, SKX 19031)	n = 6 (SK 52, SK 71, SKX ? ^b , SKX 242, SKX 308, SKX 1788)	n = 2 (SK 48, SK 85a)
<i>Homo erectus</i> (N = 9)	n = 2 (KNM-ER 820 ^c , KNM-WT 15000)	n = 2 (KNM-ER 820 ^c , KNM-WT 15000)	n = 1 (KNM-WT 15000)	n = 2 (KNM-ER 808, KNM-WT 15000)	n = 2 (Sangiran 4, KNM-WT 15000)
Early <i>Homo</i> (N = 12)	n = 2 (OH 7, STW 151)	n = 2 (OH 16, STW 151)	n = 4 (KNM-ER 1590, OH 16, StW 075, StW 151)	n = 2 (OH 16, StW 075)	n = 2 (KNM-ER 1590, SK 27)
<i>Homo naledi</i> (N = 19)	n = 2 (U.W. 101-1005c, U.W. 101-1133)	n = 4 (U.W. 101-0335, U.W. 101-0998, U.W. 101-1005b, U.W. 101-1075)	n = 3 (U.W. 101-0038, U.W. 101-0931, U.W. 101-1012)	n = 4 (U.W. 101-0073, U.W. 101-0709, U.W. 101-0932, U.W. 101-1588)	n = 6 (U.W. 101-0337, U.W. 101-0412, U.W. 101-0501, U.W. 101-706, U.W. 101-0816, U.W. 101-0908)
Neandertals (N = 35)	n = 2 (Krapina Mandible E, Le Moustier 1)	n = 6 (Krapina Mandible C, Krapina Mandible D, Krapina Mandible E, Krapina 71, Krapina 90, Le Moustier 1)	n = 7 (Krapina 123, Krapina 126, Krapina 155, Krapina 194, Krapina 195, Le Moustier 1, Gibraltar II)	n = 8 (Krapina 122, Krapina 128, Krapina 130, Krapina 131, Krapina 148, Krapina 150, Krapina 156, Le Moustier 1)	n = 12 (Krapina 56, Krapina 76, Krapina 102, Krapina 103, Krapina 141, Krapina 142, Krapina 144, Krapina 146, Krapina 191, Kulna, La Quina H5, Le Moustier 1)
Recent modern humans (N = 229)	n = 39: Inupiaq (n = 8), Newcastle Southern African (n = 16)	n = 41: Inupiaq (n = 9), Newcastle Southern African (n = 19)	n = 46: Inupiaq (n = 8), Newcastle (n = 19), Southern African (n = 19)	n = 41: Inupiaq (n = 5), Newcastle (n = 16), Southern African (n = 20)	n = 62: Inupiaq (n = 3), Newcastle (n = 39), Southern African (n = 20)

^a *Australopithecus* spp. includes 14 teeth of *A. africanus* and three teeth of *A. afarensis*.

^b Listed as "SKX ?" in Dean and Reid (2001a).

^c The perikymata counts of the antimeres of KNM-ER 820 were averaged for this analysis. All references to "KNM-ER 820" in this article refer to the average of the perikymata counts of the two antimeres for each tooth type.

perikymata on different teeth; where perikymata were denser, higher magnifications were necessary to clearly differentiate them.

D.J.R. counted perikymata in all comparative samples, but in consultation with Christopher Dean for early *Homo* and *H. ergaster/H. erectus* and in consultation with D.G.S. for Neandertals. Perikymata on the sample of *H. naledi* were counted by D.G.S. and M.C.O. An interobserver error test between D.J.R. and D.G.S. on four complete or nearly complete Neandertal crowns (selected on the basis of completeness) revealed no systematic differences across the 35 deciles over which counts were made. In other words, D.J.R. was not consistently higher in his counts than D.G.S. or vice versa. Per decile, average interobserver error between D.J.R. and D.G.S. was 1.5 perikymata. Expressed as a percentage of perikymata in each decile, on average the difference between the two observers is 10.5%. It is worth noting that Le Cabec et al. (2015:11) reported that repeated counts of perikymata per decile on synchrotron scans by the same and different observers gave "reasonable agreement," with no statistically significant mean differences among three different observers. These authors noted that variability in perikymata counts appeared to arise from several factors, including regions of the crown where perikymata are less clearly visible (owing to, for example, differential taphonomic histories) or are more difficult to clearly differentiate (such as in the cervical region).

For *H. naledi*, D.G.S. and M.C.O. first independently recorded XYZ coordinates for each perikyma on all crowns. Then, crown height measurement and decile counts were compared. If cast height measurement differences exceeded 0.5 mm, then they remeasured the crown height together and recorded that crown height. If their perikymata counts per decile differed by two or more, then they recounted that decile together. Otherwise, their counts were averaged for each decile and rounded to the nearest whole number (with 0.5 rounded up). There were deciles on some teeth for which neither D.G.S. nor M.C.O. could see perikymata clearly enough under the measuring microscope. For these teeth, D.G.S. and M.C.O. used the Leica DMS microscope to image teeth and counts were then made for the missing deciles, if perikymata could be clearly differentiated within them. Deciles were excluded from analysis if they were missing due to wear, if perikymata were not clearly visible, or if a consistent perikymata count could not be established.

2.2. Statistical analyses

Because some *H. naledi* teeth were missing perikymata counts for the first one or two cuspal deciles (Table 2), the analysis focused on comparing teeth for deciles three through 10. Only teeth with complete perikymata counts in these eight deciles were used. The number of perikymata per decile was expressed as a percentage of the total number in deciles three through 10.

A repeated measures analysis was used to analyze perikymata distribution using SAS PROC MIXED, the 'MIXED' procedure in SAS Institute 9.4. This is a likelihood-based approach that is well suited to small sample sizes, i.e., the procedure has greater power than other repeated measures analyses (SAS Institute Inc., 2008). For this analysis, the three recent modern human groups were sampled evenly and combined into one group called 'modern humans.' For each tooth type, the modern human sample was generated by randomly selecting a certain number of teeth from each group that was equivalent to the smallest group's sample size (Table 1). The modern human sample size is recorded in Table 3 and varied by tooth type (I_1 : n = 24; I_2 : n = 27; I^1 : n = 24; I^2 : n = 15; C^1 : n = 9). The heterogeneous autoregressive variance-covariance structure best fits these data. This structure makes sense for perikymata counts per decile, because it assumes that repeated measures that are closer together are more highly correlated (autoregressive) and have changing variances (heterogeneous). For each sample, the SAS

UW101-1005b

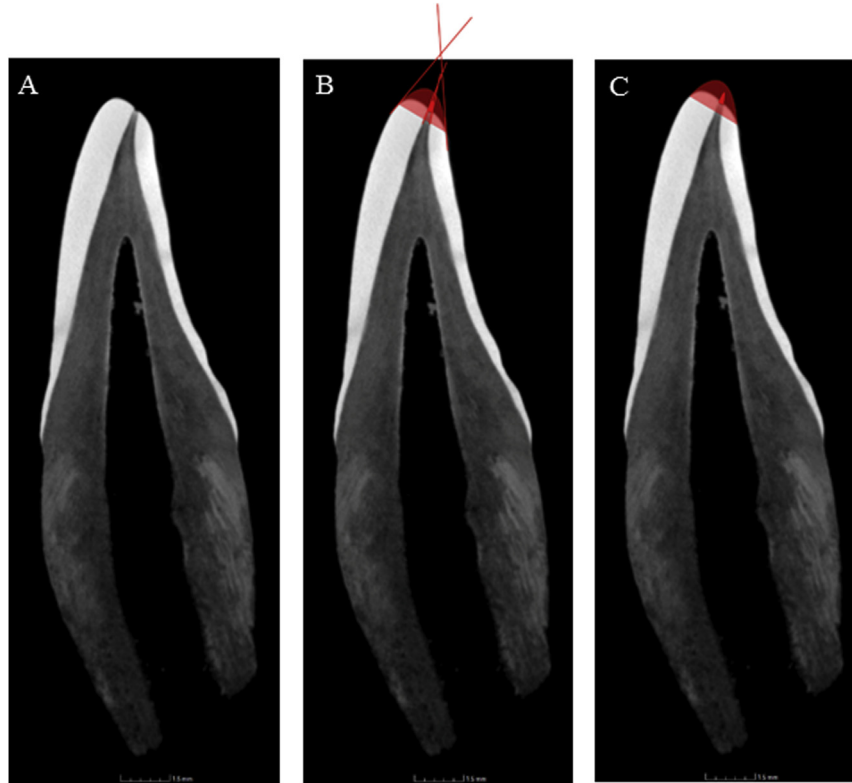


Figure 3. Method of reconstructing crown heights using the line tool on Adobe Photoshop®. A) U.W. 101-1005b (I_2) is slightly worn. B) The red lines and fill represent the area reconstructed using Adobe Photoshop®. C) The final, reconstructed, extent of the tooth that can then be measured. (For interpretation of the references to color in this figure legend, the reader is referred to the Web version of this article.)

PROC MIXED procedure gave a quadratic equation for a predicted curve representing the y-intercept (sample), slope (decile by sample interaction) and quadratic curvature (decile by decile by sample interaction). The predicted curves for each sample were compared to one another. Significant results at $\alpha = 0.05$ were subjected to a conservative Bonferroni correction, i.e., dividing 0.05 by the number of groups.

Bivariate plots of total perikymata number in deciles 3 through 10 vs. the percentage of the total number of perikymata in these deciles that are present in the cervical half (deciles 6 through 10) of the tooth are displayed for each sample for visual assessment (Table 1). This measure is similar to previous analyses in which the percentages of perikymata in the cervical half of the tooth were compared between groups (Guatelli-Steinberg et al., 2007; Xing et al., 2015). In these previous analyses, modern humans were shown to generally have a higher proportion of their total perikymata in the cervical half of the tooth as compared to earlier hominins (Guatelli-Steinberg et al., 2007, 2016; Xing et al., 2015). The only difference here is that perikymata in the cervical half of the crown are being expressed as a percentage of the total number of perikymata in deciles 3 through 10, so that no perikymata estimates from missing deciles are included. Because of this difference, the percentages of perikymata in the cervical half of the tooth reported in this paper are uniformly greater than those given in previous papers (e.g., Guatelli-Steinberg et al., 2007, 2016; Xing et al., 2015).

Finally, canonical variates analyses (CVA) were performed for each tooth type using IBM SPSS Statistics version 24. The purposes of these analyses were to: 1) assess the affinities of *H. naledi* to other groups, and 2) determine how consistently the teeth of *H. naledi* are classified as *H. naledi*. The variables were the total

number of perikymata in deciles 3 through 10 and the percentage of perikymata in the cervical half of the tooth (as above, deciles 6 through 10). In the first set of these analyses, we asked, without a priori defining *H. naledi* as its own distinct group, where each *H. naledi* tooth would be classified if it were forced to be assigned to one of the six comparative groups. The purpose of this first analysis was twofold: to assess the affinities *H. naledi* to other hominin groups and to determine whether *H. naledi* can be comfortably accommodated within existing comparative groups. In this first analysis, the groups used for classification varied by tooth type due to sample sizes (Table 4), but at maximum, those groups were *Australopithecus* spp., *P. boisei*, *P. robustus*, *H. ergaster*/*H. erectus*, Neandertals and the modern human samples (Inupiaq, northern Europeans from Newcastle-Upon-Tyne, and southern Africans). The data were transformed into discriminant functions, and group centroids were calculated. The *H. naledi* specimens were entered into the analysis as 'unknown' and were assigned to one of the comparative groups on the basis of their proximity to the nearest group centroid. Mahalanobis squared distances were recorded, and the probability that each *H. naledi* specimen actually belonged to the group with the nearest centroid was calculated. In addition, the probability that a *H. naledi* tooth could be classified into one of the a priori groups was recorded.

Next, a second canonical variates analysis was conducted, but this time with *H. naledi* designated as its own group. The data were transformed into discriminant functions, and group centroids were calculated for each group by discriminant function. To cross-validate the results of the classification, each individual was removed from the analysis, all calculations were rerun, group centroids were re-established, and then that individual was assigned a classification based on the group centroids that were

Table 2

Perikymata counts per decile from cusp tip (decile 1) to cervix (decile 10).

		Crown height (mm)	Number of perikymata per decile									
			1	2	3	4	5	6	7	8	9	10
I ₁	Mean	10.06	–	–	6.0	6.0	7.0	8.0	10.3	13.0	16.0	17.7
	SD	0.11	–	–	0.0	1.7	1.0	1.0	0.6	1.7	0.0	1.5
	U.W. 101-1005c	9.98	–	–	6	5	6	9	10	14	16	18
	U.W. 101-1133	10.14	–	–	6	5	7	7	11	14	16	16
I ₂	Mean	11.43	2.0	5.5	6.0	6.6	8.6	10.0	14.0	20.0	24.0	24.5
	SD	0.35	–	2.1	1.0	0.9	0.6	1.9	1.4	1.4	1.8	2.1
	U.W. 101-0335	11.79	–	–	6	6	8	7	13	21	22	25
	U.W. 101-0998	10.99	–	–	7	8	9	10	13	21	26	24
I ¹	Mean	11.64	–	–	6.0	8.3	11.0	11.3	13.4	16.0	19.0	20.7
	SD	0.40	–	–	1.7	1.2	2.0	2.5	1.2	1.7	1.7	1.5
	U.W. 101-0038	11.74	–	–	7	9	11	11	13	15	18	19
	U.W. 101-0931	11.20	–	–	4	9	9	9	13	18	18	22
I ²	Mean	8.79	–	4.7	5.6	6.0	7.0	9.0	12.4	14.4	16.2	16.6
	SD	0.46	–	0.6	0.9	1.4	1.0	1.2	1.1	3.1	4.1	2.3
	U.W. 101-0073	8.45	–	5	6	5	6	9	12	12	15	16
	U.W. 101-0709	8.50	–	–	6	7	8	10	12	16	18	19
C ¹	Mean	13.06	4.0	5.0	6.5	8.5	8.7	12.3	17.0	19.2	21.0	21.0
	SD	0.52	1.4	0.8	1.1	1.2	1.5	3.2	2.3	1.5	1.8	2.7
	U.W. 101-0337	13.01	–	–	7	7	10	11	17	19	22	23
	U.W. 101-0412	13.74	–	–	7	8	7	9	14	17	18	24
C ¹	Mean	12.60	3	5	8	10	10	13	15	21	21	22
	SD	12.53	–	6	6	10	10	13	17	20	22	20
	U.W. 101-0706	12.53	–	6	6	10	10	13	17	20	22	20
	U.W. 101-0816	12.82	5	4	6	8	8	10	20	20	23	19
C ¹	Mean	13.65	–	5	5	8	7	18	19	18	20	18
	SD	13.65	–	5	5	8	7	18	19	18	20	18

Table 3Sample of *Homo naledi* and comparative taxa used for the PROC MIXED regression analysis.

	Total (n)	I ₁	I ₂	I ¹	I ²	C ¹
<i>Homo naledi</i>	19	n = 2	n = 4	n = 3	n = 4	n = 6
<i>Australopithecus</i> spp.	16	n = 3	–	n = 5	n = 5	n = 3
<i>Paranthropus boisei</i>	4	n = 4	–	–	–	–
<i>Paranthropus robustus</i>	21	n = 4	n = 2	n = 7	n = 6	n = 2
<i>Homo erectus</i>	8	n = 2	n = 2	–	n = 2	n = 2
Neandertals	35	n = 2	n = 6	n = 7	n = 8	n = 12
Recent modern humans	99	n = 24 (8 per group)	n = 27 (9 per group)	n = 24 (8 per group)	n = 15 (5 per group)	n = 9 (3 per group)

Table 4Sample of *Homo naledi* and comparative taxa used for the canonical variates analysis. 'MH' refers to recent modern humans.

	Total (N)	I ₁	I ₂	I ¹	I ²	C ¹
<i>Homo naledi</i>	19	n = 2	n = 4	n = 3	n = 4	n = 6
<i>Australopithecus</i> spp.	16	n = 3	–	n = 5	n = 5	n = 3
<i>Paranthropus boisei</i>	4	n = 4	–	–	–	–
<i>Paranthropus robustus</i>	21	n = 4	n = 2	n = 7	n = 6	n = 2
<i>Homo erectus</i>	8	n = 2	n = 2	–	n = 2	n = 2
Neandertals	35	n = 2	n = 6	n = 7	n = 8	n = 12
MH: Inupiaq	33	n = 8	n = 9	n = 8	n = 5	n = 3
MH: Newcastle	102	n = 15	n = 13	n = 19	n = 16	n = 39
MH: Southern African	94	n = 16	n = 19	n = 19	n = 20	n = 20

created without that individual's influence. This procedure, called leave-one-out (or jackknifed) cross-validation, is done through as many iterations as individuals in the total sample.

3. Results

Table 5 summarizes the results of the SAS PROC MIXED repeated measures regression analyses. For each tooth type, there were four to six comparisons. When the sample size for a species was one

($n = 1$), it was not included in the analysis. *H. habilis*/*H. rudolfensis* was not included in the statistical analysis, owing to small sample sizes and uncertainties of classification for some specimens; however, graphs of the individual specimens are included in SOM Figure S1. Comparison of *H. naledi* to *Australopithecus*, *P. robustus*, *P. boisei*, *H. ergaster*/*H. erectus*, Neandertals and modern humans varied by tooth type. That is, for some tooth types (e.g., I₁), comparisons of *H. naledi* to all of these taxa/groups were possible, but for other tooth types (e.g., I₂), sample sizes limited the number of groups/taxa to which *H. naledi* could be compared. Equal numbers of specimens belonging to each modern human group (Newcastle, Inupiaq, and southern African) comprised the combined 'modern human' samples.

As is evident in Table 5, statistically significant differences between *H. naledi* and the other hominin samples (at the conventional $p < 0.05$ and using a conservative Bonferroni correction) vary by tooth type. Where there are statistically significant differences, they most often relate to quadratic curvature. The I₂ of *H. naledi* is especially notable in this regard, as its quadratic curvature coefficient is significantly different from that of all the other hominin I₂. In most cases (with the exception of the C¹), the sign of the quadratic coefficient in *H. naledi* is positive, while the sign of the quadratic coefficients of the other extinct hominins tends to be

Table 5
Results of the PROC MIXED regression analyses, by comparing each model estimate to the *Homo naledi* model^a.

	n	Y-intercept		Slope		Quadratic curvature	
		Estimate	p	Estimate	p	Estimate	p
I₁							
<i>H. naledi</i>	2	5.38	0.006 ^{a,c}	0.45	0.591 ^a	0.20	0.022 ^{a,b}
<i>Australopithecus</i> spp.	3	3.97	0.549	2.29	0.085	-0.07	0.017 ^b
<i>P. boisei</i>	4	6.66	0.564	0.65	0.838	0.11	0.415
<i>P. robustus</i>	4	8.76	0.128	1.47	0.314	-0.11	0.004 ^c
<i>H. erectus</i>	2	5.17	0.938	2.22	0.131	-0.10	0.014 ^b
Neandertals	2	5.36	0.994	2.15	0.145	-0.10	0.015 ^b
Modern humans	24	4.52	0.650	2.01	0.067	-0.04	0.007 ^c
I₂							
<i>H. naledi</i>	4	3.72	0.019 ^{a,b}	0.75	0.257 ^a	0.21	0.002 ^{a,c}
<i>P. robustus</i>	2	5.54	0.490	2.23	0.192	-0.12	0.005 ^c
<i>H. erectus</i>	2	4.58	0.743	2.48	0.127	-0.13	0.004 ^c
Neandertals	6	4.76	0.597	2.62	0.027 ^b	-0.16	<0.001 ^c
Modern humans	27	4.38	0.686	2.32	0.025 ^b	-0.09	<0.001 ^c
I¹							
<i>H. naledi</i>	3	4.43	0.006 ^{a,c}	1.52	0.192 ^a	0.05	0.456 ^a
<i>Australopithecus</i> spp.	5	4.87	0.820	3.19	0.036 ^b	-0.26	<0.001 ^c
<i>P. robustus</i>	7	9.25	0.008 ^c	0.94	0.434	-0.04	0.261
Neandertals	7	9.07	0.011 ^c	0.67	0.252	0.02	0.683
Modern humans	24	3.54	0.581	2.95	0.033 ^b	-0.17	0.002 ^c
I²							
<i>H. naledi</i>	4	3.24	0.014 ^{a,b}	1.71	0.003 ^{a,c}	0.06	0.271 ^a
<i>Australopithecus</i> spp.	5	4.86	0.337	2.97	0.084	-0.22	<0.001 ^c
<i>P. robustus</i>	6	7.50	0.009 ^c	2.22	0.465	-0.20	<0.001 ^c
<i>H. erectus</i>	2	6.57	0.1263	2.41	0.453	-0.19	0.009 ^c
Neandertals	8	8.35	0.001 ^c	0.91	0.228	0.003	0.391
Modern humans	15	4.64	0.319	1.87	0.790	-0.02	0.185
C¹							
<i>H. naledi</i>	6	2.51	0.016 ^{a,b}	2.44	<0.001 ^{a,c}	-0.04	0.421 ^a
<i>Australopithecus</i> spp.	3	5.74	0.057	2.73	0.707	-0.22	0.031 ^b
<i>P. robustus</i>	2	0.73	0.365	5.31	0.002 ^c	-0.48	<0.001 ^c
<i>H. erectus</i>	2	7.14	0.019 ^b	1.78	0.467	-0.11	0.486
Neandertals	12	8.06	<0.001 ^c	1.33	0.046 ^b	-0.06	0.698
Modern humans	9	5.05	0.045 ^b	1.94	0.396	-0.05	0.835

^a Significance of the *H. naledi* model estimate. All other *p*-values compare the other model estimates to *H. naledi*.

^b Significant at $\alpha = 0.05$.

^c Significant with a Bonferroni correction (calculated by dividing 0.05 by the number of populations measured in each tooth type).

negative (exceptions are the Neandertal I¹ and I², and the *P. boisei* I₁), suggesting that the *H. naledi* curves tend to have less downward curvature than the extinct hominin samples. Although modern human quadratic curvatures have negative values, in some cases they are close to zero (for all but the I¹), and in this respect the modern human sample is somewhat more like *H. naledi* than are the other hominin samples.

The graphs of the predicted growth curves (Fig. 4) reflect this difference in curvature. Indeed, *H. naledi* has very little curvature (either upward or downward) in the predicted growth curve for all upper anterior tooth types (C¹, I¹, and I²), while for I₁ and I₂, the growth curves appear to have a slightly upward (positive) curvature, i.e., they exhibit a non-linear increase in perikymata numbers in the cervical deciles. These growth curve differences reflect the fact that the percentage of perikymata in early (cuspal) deciles in *H. naledi* teeth is much lower than the percentage found in later (cervical) deciles. Inspection of the predicted growth curves in Figure 4 indicates that this differential between cuspal and cervical deciles is greater for *H. naledi* than it is for the other extinct hominins. Modern humans tend to differ from the other extinct hominins in a similar way: they too tend to show a strong gradient from their cuspal to cervical deciles in the percentages of perikymata present within them. Yet, to varying degrees per tooth type, *H. naledi* seems to show an even stronger gradient than do modern humans. Indeed, statistically significant differences between *H. naledi* and modern humans were found for quadratic curvature in the I¹, I₁, and I₂. Figure 5 gives an example of perikymata

distribution on a lower lateral incisor of *H. naledi*. Additional examples are provided in SOM Figures S6–S9. Visually, it is quite clear that perikymata are extremely widely spaced in earlier deciles relative to later deciles.

The bivariate plots of percentage of perikymata in the cervical half of the tooth (deciles 6 through 10 divided by the sum of perikymata in deciles 3 through 10) vs. the total number of perikymata (sum of perikymata in deciles 3 through 10) for all samples are shown in Figure 6. In most cases, *H. naledi* appears at the top of modern human ranges (or exceeds them) for percentage of perikymata in the cervical half of the tooth, but falls in the middle to lower end of modern human ranges for perikymata number. Descriptive statistics corresponding to these bivariate plots are included in SOM Table S2.

Results from the first set of CVA are in Tables 6 and 7. When entered as 'unknown,' the *H. naledi* teeth were classified based on their proximity to the nearest group centroid. On this basis, they were classified into Newcastle in one instance, *P. robustus* in one instance, *P. boisei* in two instances, and in southern African for the remainder (Table 6). However, for eight of the 19 *H. naledi* individuals, it was significantly unlikely ($p < 0.05$) that the teeth actually belonged to those groups with the nearest centroids. Table 7 lists the probability of each *H. naledi* tooth falling into each of the different groups, when forced to be assigned to one of them. To interpret these results, consider the case of the *H. naledi* I². All of the *H. naledi* I²s fall beyond the recorded modern human range of variation on the bivariate plots (Fig. 6). The same data used to create

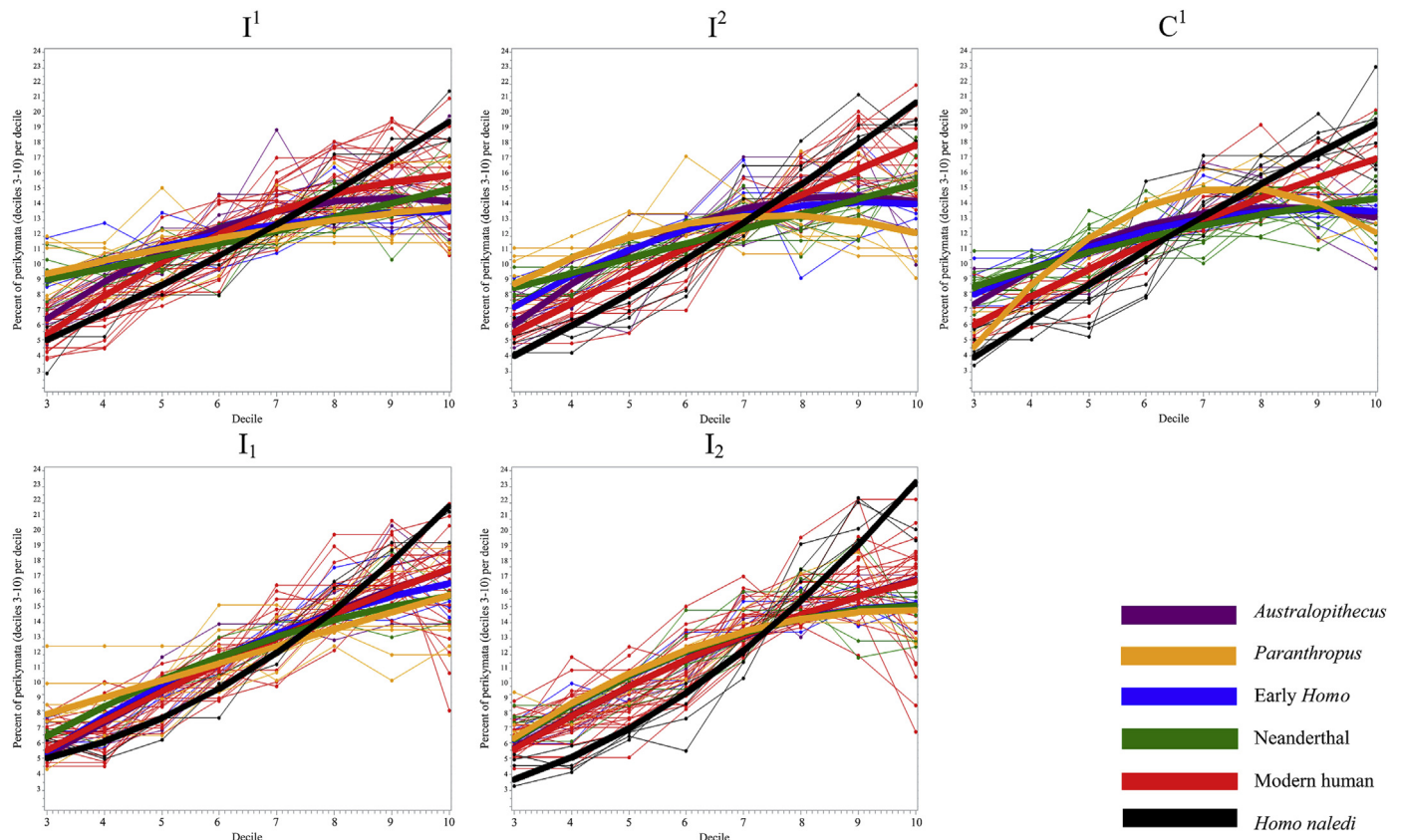


Figure 4. The distribution of perikymata (percent of perikymata per decile) for deciles 3–10 by tooth type and group. Thick, continuous lines represent the predicted growth curves modeled by the SAS PROC MIXED analysis for each group. Thin, jointed lines represent individual repeated measures for each tooth's percent of perikymata per decile. Note that the *Australopithecus* I_2 model curve is located just behind the MH curve.

the bivariate plots form the basis of the CVA. The *H. naledi* I^2 teeth are closer to the modern human teeth than they are to those of any other group, thus making clear why they are most likely to be assigned to modern humans. Table 7 supports this with very high probability scores (ranging from 0.769 to 0.978) for classifying *H. naledi* in the southern African group as compared to the other groups. As shown in Table 6, the four *H. naledi* I^2 s all showed greatest proximity to the group centroid of modern human southern Africans; yet, in three of these four cases, they were significantly unlikely to actually belong to this group (Table 6).

When modern humans are combined into a single group (SOM Table S3), the *H. naledi* teeth were classified into *P. boisei* in two instances and all the rest were classified as modern human. For seven of the 19 *H. naledi* individuals, it was significantly unlikely that the teeth could have actually belonged to the group they were classified as (SOM Table S4). SOM Table S5 lists the probability of each *H. naledi* tooth falling into each group; again, the probabilities for modern humans tend to be highest.

The second set of canonical variates analysis, the cross-validated CVA, revealed that 13 of the 19 *H. naledi* teeth were correctly classified as such (68%; Table 8). Six teeth (32%) of the *H. naledi* sample were identified as belonging to another group/taxon than *H. naledi*: one I_1 was classified as *P. boisei*, one C^1 was classified as Newcastle modern human, and one I_2 and all three I^1 were classified as southern African modern human. Six out of the 313 comparative teeth in the subsample used for this analysis (1.9% of the comparative sample) were misclassified as *H. naledi*, all of which were modern human teeth (two from Newcastle and four from southern Africa). *H. naledi* was never classified as *Australopithecus*, *P. robustus*, *H. ergaster/H. erectus* or Neanderthal, and no

teeth from those groups were ever classified as *H. naledi*. Correct group classification (for all groups) obtained by the cross-validated procedure ranges from 52.7% (I_2) to 58.6% (C^1). Note that this classification is based on separating the modern human groups. When modern humans are combined into a single group (SOM Table S3), the cross-validation improves, ranging from 61.8 to 73.2% (SOM Table S6). This improvement reflects the larger sample size and range of variation of the modern human group, which results in modern human teeth being consistently classified as such. As might be expected, given the overlap in modern human ranges on the bivariate plots, correct group classification obtained by the cross-validated procedure improved when modern humans were combined into one group, from 61.8% (C^1) correctly classified to 73.2% (I_1 and I_2) correctly classified.

4. Discussion

The analyses conducted here reveal that relative to both modern humans and earlier hominins, the anterior teeth of *H. naledi* tend to exhibit greater percentage increases in perikymata number across deciles of crown height (from cusp to cervix). Thus, when the percentages of perikymata per decile are plotted from deciles 3 to 10 for different hominin taxa, predicted curves for *H. naledi* often exhibit statistically significant differences from other taxa in quadratic curvature. *Homo naledi* predicted curves often show either minimal curvature or positive curvature (Fig. 4). Predicted curves for the comparative samples are more likely to exhibit negative curvature, reflecting a greater tendency for perikymata numbers to plateau rather than continue to increase across deciles, as they do in *H. naledi*. The most

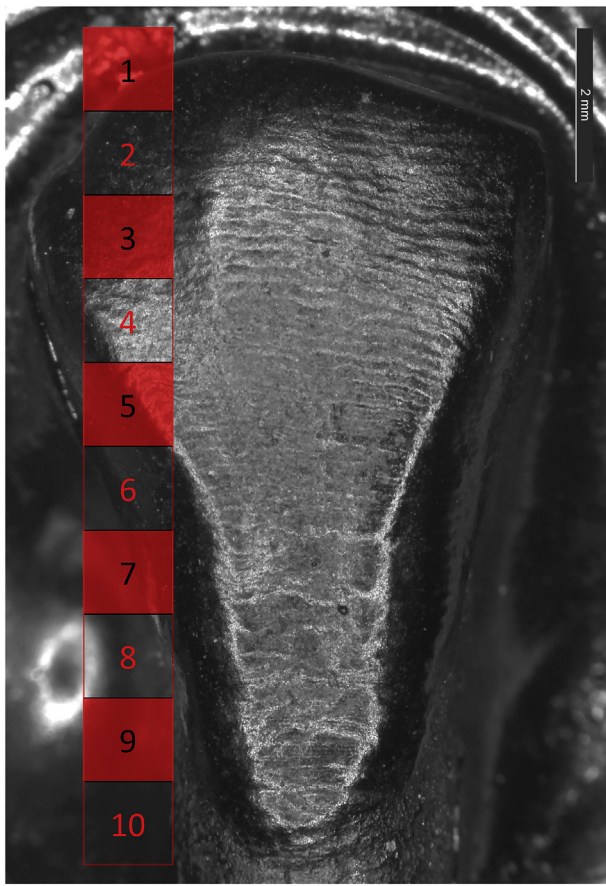


Figure 5. Lateral view of U.W. 101-1005b (I_2). The enlarged image demonstrates the very tightly packed perikymata in the cervical deciles compared to the much more widely spaced perikymata toward the cusp tip. See SOM Figures S6–S9 for additional examples.

distinctive difference in quadratic curvature is for the I_2^1 , for which *H. naledi* is statistically significantly different (with Bonferroni correction) from *P. robustus*, *H. ergaster/H. erectus*, Neandertals and extant modern humans. The least distinctive difference is for the C^1 , for which there is only one statistically significant difference in quadratic curvature, and that is between *H. naledi* and *P. robustus*. Although modern humans have negative quadratic curvatures, for most tooth types (with the exception of I^1) their magnitudes are close to zero. Thus, like *H. naledi*, modern humans exhibit a strong gradient in the distribution of perikymata from cusp to cervix. However, unlike *H. naledi*, modern humans display gradients that are somewhat less pronounced. As noted, for three tooth types (I_1 , I_2 , and the I^1), even though the quadratic coefficient differences between *H. naledi* and modern humans were small in magnitude, they were significantly different.

Plotting the percentage of perikymata in the cervical half of the tooth (relative to the total number of perikymata between deciles 3 and 10; Fig. 6) revealed that *H. naledi* tends to fall into the upper left (I_1 , I_2^1) to upper middle (I_2 , C^1 , I^1) regions of these graphs. We note that for the I^1 , with a sample size of three, the hypoplastic defect in the cervical region of U.W. 101-1012 must have some effect on the perikymata count in the cervical half of this tooth. Thus, the I^1 position of *H. naledi* on this graph may be expected to shift somewhat as more samples of *H. naledi* I^1 become available. In general, the position of *H. naledi* on these graphs reflects its relatively high percentage of perikymata in the cervical region of the tooth, at the top of or exceeding modern human ranges, combined with its relatively low to mid-range total

number of perikymata (Fig. 6). In this regard, for some tooth types (especially I_1 and I_2^1), *H. naledi* might be said to reverse the Neandertal condition, in which there are relatively low percentages of perikymata in the cervical regions of teeth paired with total perikymata numbers that fall well within modern human ranges. Thus, the present results further support the view that the distribution of perikymata in teeth can evolve independently of the total number of perikymata in tooth crowns. Modern human teeth with more perikymata tend to pack them preferentially in their cervical regions, such that perikymata number and distribution tend to be correlated within our species (Reid and Ferrell, 2006). Dissociation between perikymata number and perikymata distribution only becomes evident when comparisons are made across taxa.

The purpose of performing the CVA in this study was to assess the affinities and taxonomic distinctiveness of *H. naledi*. Results vary by tooth type, but the I^2 provides an instructive example. All four of these *H. naledi* teeth were classified as southern African when *H. naledi* was entered as unknown (Tables 6 and 7) and three of the four were classified as southern African in the cross-validated analysis (Table 8). However, three of the four *H. naledi* I^2 were significantly unlikely to actually belong to the southern African group on the basis of proximity to its centroid (Table 6). This suggests that *H. naledi* I^2 are generally distinct from those of southern Africans, but that of all the comparative samples, southern Africans show the least difference from *H. naledi*. The CVA analyses therefore mirror the repeated measures analyses. Together these analyses suggest that the combination of relatively low/middle total perikymata numbers with relatively high percentages of perikymata in the cervical region is more often found in *H. naledi* than in other hominins.

The cross-validation results of the CVA suggest that the combination of perikymata number and percentage of perikymata in the cervical half of the tooth can moderately discriminate among hominin species (Table 8). Only moderate discrimination was expected, as it has been noted that there is overlap among taxa when they are compared for these two variables (Xing et al., 2015) and the bivariate plots clearly reveal that overlap (Fig. 6). However, it is important to note that what is primarily causing the misclassifications is the southern African sample, which is quite variable for perikymata number and percent perikymata in the cervical region of the crown. This can be seen in Tables 6, 7, SOM Tables S3–S7, and Figure 6, where there is a noticeable degree of overlap between southern Africans and all other groups. It is also important to remember that other aspects of variation in perikymata distribution—particularly patterns of distribution by decile—are not included in the CVA but can differ among species. For example, all three *H. naledi* I^1 s were classified as modern humans, but the SAS PROC MIXED predicted curves for *H. naledi* and modern human I^1 s differed significantly in their quadratic curvatures (Table 5 and Fig. 4).

The somewhat greater affinity of *H. naledi* to modern humans, and particularly to southern Africans, would seem to have to do not only with the variability of the southern African sample, but also with the strong gradient in perikymata distribution that modern humans exhibit from cusp to cervix. This is a feature that *H. naledi* shares with modern humans but tends to exhibit to a greater degree (especially for the I^1 , I_1 , and I_2 , as noted earlier). Similarities to southern Africans should not be overstated, given that there were significant differences between *H. naledi* and southern Africans in different sets of analyses. Given that histological analyses that could sort out homoplasies in perikymata number and distributions have yet to be accomplished, it seems premature to speculate about the causes of the greater affinity of *H. naledi* to southern Africans than to other hominins.

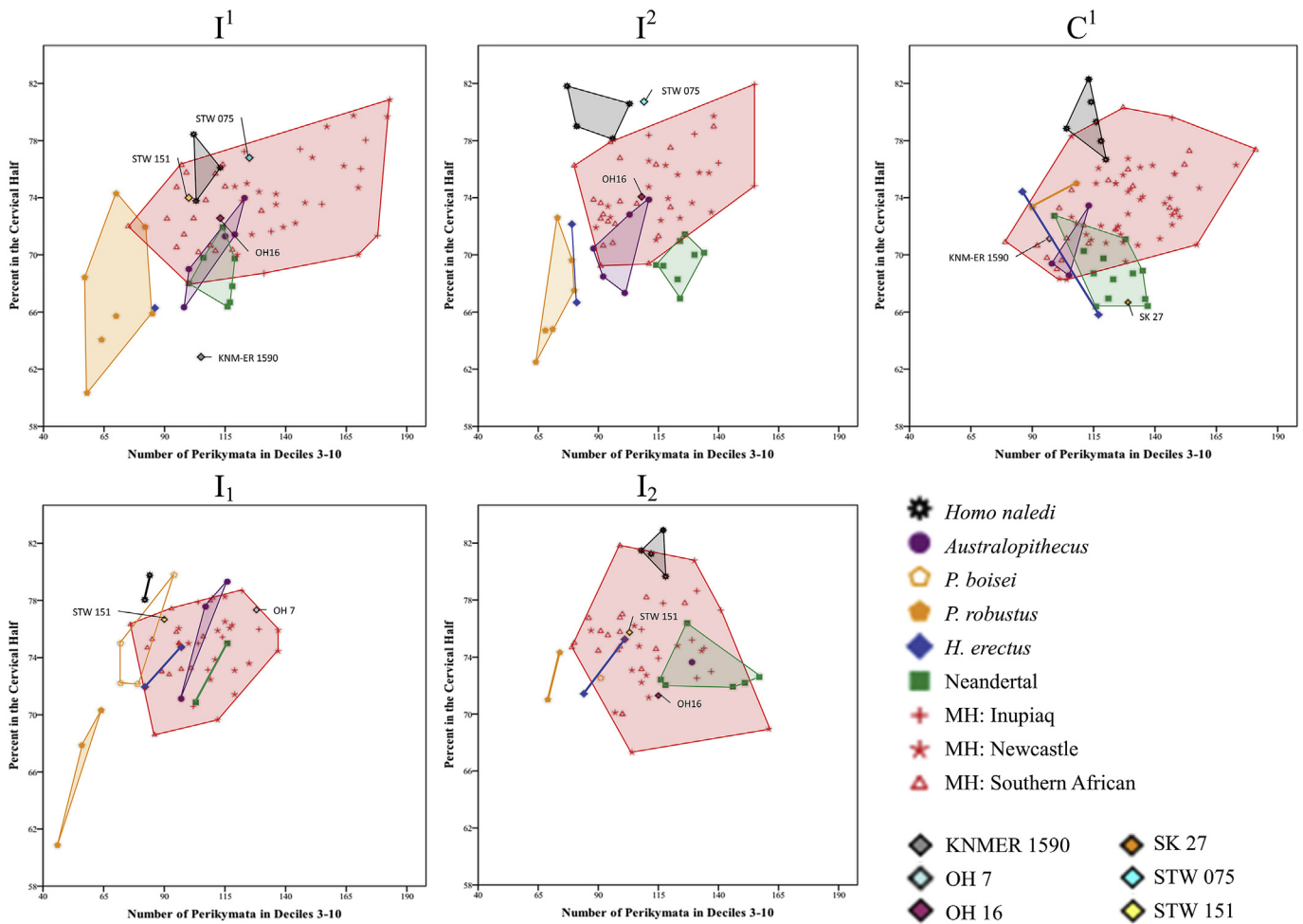


Figure 6. Bivariate plots of the total number of perikymata in deciles 3–10 and the percent of that total found in the cervical half of the tooth (deciles 6–10). Fossils of unknown or contested species designation are marked individually.

Table 6

Classification of *Homo naledi* individuals in the first canonical variates analysis, in which *H. naledi* is not a priori defined. This table shows the probability that each individual tooth of *H. naledi* belongs to the group with the nearest centroid. 'MH' refers to recent modern humans.

	Nearest group centroid	Squared Mahalanobis distance to centroid	<i>p</i>
I_1			
UW101-1005c	<i>Paranthropus boisei</i>	3.355	0.187
UW101-1133	<i>Paranthropus boisei</i>	1.462	0.481
I_2			
UW101-0335	MH: Southern African	5.351	0.069
UW101-0998	MH: Southern African	4.214	0.122
UW101-1005b	MH: Southern African	5.410	0.067
UW101-1075	MH: Southern African	9.088	0.011 ^a
I^1			
UW101-0038	MH: Southern African	0.137	0.934
UW101-1012	MH: Southern African	1.148	0.553
UW101-0931	MH: Southern African	4.033	0.133
I^2			
UW101-0073	MH: Southern African	9.780	0.008 ^a
UW101-0709	MH: Southern African	3.978	0.137
UW101-1588	MH: Southern African	19.090	<0.001 ^a
UW101-0932	MH: Southern African	7.563	0.023 ^a
C^1			
UW101-0337	MH: Southern African	6.357	0.042 ^a
UW101-0412	MH: Southern African	7.395	0.025 ^a
UW101-0501	MH: Newcastle, UK	2.927	0.231
UW101-0706	MH: Southern African	3.731	0.155
UW101-0816	MH: Southern African	9.809	0.007 ^a
UW101-0908	<i>Paranthropus robustus</i>	9.645	0.008 ^a

^a Significant at $\alpha = 0.05$.

Table 7
The probability that each *Homo naledi* specimen could have been assigned to groups classified in the canonical variates analysis (Table 6). 'MH' refers to recent modern humans.

	<i>Australopithecus</i> spp.	<i>P. boisei</i>	<i>P. robustus</i>	<i>H. erectus</i>	Neandertals	MH: Inupiaq	MH: Newcastle	MH: S. African	Sum of probabilities
I₁									
UW101-1005c	0.009	0.590	0.000	0.026	0.000	0.003	0.000	0.372	1.000
UW101-1133	0.007	0.552	0.000	0.037	0.000	0.003	0.000	0.399	1.000
I₂									
UW101-0335	–	–	0.000	0.008	0.004	0.178	0.075	0.734	1.000
UW101-0998	–	–	0.000	0.006	0.024	0.402	0.151	0.417	1.000
UW101-1005b	–	–	0.000	0.007	0.007	0.265	0.093	0.628	1.000
UW101-1075	–	–	0.000	0.003	0.008	0.420	0.067	0.502	1.000
I¹									
UW 101-0038	0.082	–	0.014	–	0.034	0.002	0.018	0.849	1.000
UW 101-1012	0.061	–	0.002	–	0.019	0.010	0.075	0.833	1.000
UW 101-0931	0.017	–	0.003	–	0.002	0.001	0.010	0.967	1.000
I²									
UW101-0073	0.007	–	0.001	0.008	0.000	0.000	0.030	0.954	1.000
UW101-0709	0.012	–	0.000	0.003	0.000	0.004	0.129	0.853	1.000
UW101-1588	0.002	–	0.000	0.003	0.000	0.000	0.017	0.978	1.000
UW101-0932	0.004	–	0.000	0.000	0.000	0.032	0.195	0.769	1.000
C¹									
UW101-0337	0.005	–	0.146	0.002	0.000	0.102	0.321	0.424	1.000
UW101-0412	0.007	–	0.315	0.004	0.000	0.052	0.217	0.405	1.000
UW101-0501	0.010	–	0.045	0.005	0.003	0.064	0.465	0.408	1.000
UW101-0706	0.007	–	0.083	0.003	0.001	0.082	0.397	0.427	1.000
UW101-0816	0.003	–	0.244	0.001	0.000	0.119	0.241	0.393	1.000
UW101-0908	0.001	–	0.364	0.001	0.000	0.138	0.166	0.330	1.000

In light of speculation by some paleoanthropologists that *H. naledi* may be a form of *H. erectus* (see Randolph-Quinney, 2015), it is worth noting that *H. erectus*/*H. ergaster* is never classified as *H. naledi* or vice versa. In this study, there is only one tooth of Asian *H. erectus* included in the sample (Sangiran 4, C¹), so comparisons are most often between *H. naledi* and *H. ergaster*. That *H. naledi* separates from *H. ergaster* in the present study supports the view that *H. naledi* is not simply a late surviving African form of *H. erectus*. However, it should be noted that the sample size for *H. erectus* is small ($n = 9$ teeth) and, as previously noted, includes teeth from some individuals (e.g., KNM-ER 820) for which perikymata are not as distinct at the cervix as they are in other individuals (e.g., KNM-WT 15000). That Neandertals and *H. naledi* were never classified as each other is also of note, not because *H. naledi* has ever been claimed to be similar to Neandertals, but because Neandertals tend to exhibit the reverse combination of perikymata number and percentage of perikymata in the cervical region that *H. naledi* does.

Overall, the analyses in this study characterize patterns of enamel growth by species as assessed from the enamel surface, with a particular focus on *H. naledi*. This study leaves the question open as to the specific enamel growth processes that underlie species differences in enamel growth. As noted earlier, within humans, differences between individuals in perikymata distribution across deciles are related to differences in extension rates across these same deciles (Guatelli-Steinberg et al., 2012). Those with a greater difference in perikymata number between earlier-forming and later-forming deciles exhibit a greater decline in extension rates across these deciles (Guatelli-Steinberg et al., 2012). To the degree that perikymata distribution reflects rates of enamel extension in *H. naledi*, then it would seem that, somewhat like modern humans, extension rates per decile are high early in crown formation in *H. naledi* and drop rapidly as ameloblasts continue to differentiate toward the cervix. However, as secretion rates and the surface contour of a tooth can affect perikymata distribution as well, examining these additional variables will be necessary to definitively establish the causes of *H. naledi*'s perikymata distribution pattern.

In terms of perikymata numbers, *H. naledi* tends toward the low to middle range of hominin (including modern human) values. The

total number of perikymata on a tooth is related to total time it takes for the tooth's lateral enamel to form, as lateral enamel formation time is the product of periodicity times total perikymata number. To obtain periodicities for *H. naledi*, actual or virtual histology will be necessary. If *H. naledi* has periodicities that are like those of modern humans, then this would suggest that lateral enamel formation is somewhat shorter in *H. naledi* relative to most modern humans, or at least at the shorter end of the modern human range. Given the small anterior tooth size of *H. naledi* (Berger et al., 2015; Deleuzene et al., 2016), relatively short lateral enamel formation times would not be surprising. *P. robustus*, like *H. naledi*, has small anterior teeth, and forms its lateral enamel in short periods of time (Dean et al., 2001). However, the teeth of *P. robustus* seem to form in a way that is quite different from those of *H. naledi*; in the former, perikymata are distributed nearly evenly along the lateral enamel surface (Beynon and Wood, 1987; Le Cabec et al., 2015; Fig. 4), while in the latter there is a steep gradient in perikymata distribution. Thus, the way that perikymata are distributed along the lateral enamel surfaces of hominin anterior tooth crowns seems unrelated to tooth size.

To the extent that perikymata per decile reflect extension rates per decile (though it must be kept in mind that they can be affected by other factors) and number of perikymata per tooth is related to lateral enamel formation time, the dissociation of perikymata distribution and total perikymata number across species should be expected. Total enamel formation times and rates of enamel extension per decile are themselves dissociated across hominin species (Dean, 2009). That is because total enamel formation time depends not only on the rates of enamel extension but also on when enamel formation terminates. In other words, rates of enamel formation and the total duration of enamel formation are not necessarily linked.

Further work on enamel growth in *H. naledi* should help to elucidate the patterns described here. If fine microstructural features are well-preserved in the *H. naledi* teeth, virtual or actual histology will make it possible to assess the specific enamel growth processes that underlie how perikymata are distributed in *H. naledi* and the length of time it took to form lateral (as well as cuspal) enamel on these teeth. In addition, it should be possible to use information gained from histological examination to assess age at

Table 8

Cross-validated canonical variates analysis results. 'MH' refers to recent modern humans.

I_1^a	Predicted group membership								Total	
	<i>H. naledi</i>	<i>Australopithecus</i> spp.	<i>P. boisei</i>	<i>P. robustus</i>	<i>H. erectus</i>	Neandertals	MH: Inupiaq	MH: Newcastle		MH: S. African
<i>H. naledi</i>	1 (50%)		1 (50%)							2 (100%)
<i>Australopithecus</i> spp.						1 (33.3%)		2 (66.7%)		3 (100%)
<i>P. boisei</i>			2 (50%)					2 (50%)		4 (100%)
<i>P. robustus</i>				4 (100%)						4 (100%)
<i>H. erectus</i>								2 (100%)		2 (100%)
Neandertals								2 (100%)		2 (100%)
MH: Inupiaq								5 (62.5%)	3 (37.3%)	8 (100%)
MH: Newcastle						1 (6.7%)		12 (80%)	2 (13.3%)	15 (100%)
MH: S. African			1 (6.3%)			3 (18.8%)			12 (75%)	16 (100%)
I_2^b	Predicted group membership							Total		
	<i>H. naledi</i>	<i>P. robustus</i>	<i>H. erectus</i>	Neandertals	MH: Inupiaq	MH: Newcastle	MH: S. African			
<i>H. naledi</i>	4 (100%)							4 (100%)		
<i>P. robustus</i>		1 (50%)					1 (50%)	2 (100%)		
<i>H. erectus</i>							2 (100%)	2 (100%)		
Neandertals				3 (50%)	1 (16.7%)	2 (33.3%)		6 (100%)		
MH: Inupiaq				1 (11.1%)	4 (44.4%)	2 (22.2%)	2 (22.2%)	9 (100%)		
MH: Newcastle	1 (7.7%)			1 (7.7%)	2 (15.4%)	4 (30.8%)	5 (38.5%)	13 (100%)		
MH: S. African	1 (5.3%)				1 (5.3%)	4 (21.1%)	13 (68.4%)	19 (100%)		
I_1^c	Predicted group membership							Total		
	<i>H. naledi</i>	<i>Australopithecus</i> spp.	<i>P. robustus</i>	Neandertals	MH: Inupiaq	MH: Newcastle	MH: S. African			
<i>Homo naledi</i>							3 (100%)	3 (100%)		
<i>Australopithecus</i> spp.				1 (20%)			4 (80%)	5 (100%)		
<i>P. robustus</i>			5 (71.4%)				2 (28.6%)	7 (100%)		
Neandertal				4 (57.1%)			3 (42.9%)	7 (100%)		
MH: Inupiaq				1 (12.5%)		6 (75%)	1 (12.5%)	8 (100%)		
MH: Newcastle				1 (5.3%)	1 (5.3%)	14 (73.7%)	3 (28.6%)	19 (100%)		
MH: S. African				2 (10.5%)		1 (5.3%)	16 (84.2%)	19 (100%)		
I_2^d	Predicted group membership								Total	
	<i>H. naledi</i>	<i>Australopithecus</i> spp.	<i>P. robustus</i>	<i>H. erectus</i>	Neandertals	MH: Inupiaq	MH: Newcastle	MH: S. African		
<i>Homo naledi</i>	3 (75%)							1 (25%)	4 (100%)	
<i>Australopithecus</i> spp.		1 (20%)			1 (20%)			3 (60%)	5 (100%)	
<i>P. robustus</i>			5 (83.3%)					1 (16.7%)	6 (100%)	
<i>H. erectus</i>			1 (50%)					1 (50%)	2 (100%)	
Neandertals					8 (100%)				8 (100%)	
MH: Inupiaq					1 (20%)	1 (20%)	2 (40%)	1 (20%)	5 (100%)	
MH: Newcastle					1 (6.3%)	1 (6.3%)	9 (56.3%)	5 (31.3%)	16 (100%)	
MH: S. African	2 (10%)	1 (5%)			1 (5%)	1 (5%)	4 (20%)	11 (55%)	20 (100%)	
C_1^e	Predicted group membership								Total	
	<i>H. naledi</i>	<i>Australopithecus</i> spp.	<i>P. robustus</i>	<i>H. erectus</i>	Neandertals	MH: Inupiaq	MH: Newcastle	MH: S. African		
<i>Homo naledi</i>	5 (83.3%)						1 (16.7%)		6 (100%)	
<i>Australopithecus</i> spp.					1 (33.3%)		2 (66.6%)		3 (100%)	
<i>P. robustus</i>								2 (100%)	2 (100%)	
<i>H. erectus</i>			1 (50%)		1 (50%)				2 (100%)	
Neandertals					8 (66.7%)		3 (25%)	1 (8.3%)	12 (100%)	
MH: Inupiaq							3 (100%)		3 (100%)	
MH: Newcastle	1 (2.6%)				2 (5.1%)		34 (87.2%)	2 (5.1%)	39 (100%)	
MH: S. African	1 (5%)						15 (75%)	4 (20%)	20 (100%)	

^a 55.4% of cross-validated grouped cases correctly classified.^b 52.7% of cross-validated grouped cases correctly classified.^c 57.4% of cross-validated grouped cases correctly classified.^d 57.6% of cross-validated grouped cases correctly classified.^e 58.6% of cross-validated grouped cases correctly classified.

death in juvenile members of this species, and then to compare their overall rates and pattern of dental development with that of modern humans and other fossil hominin groups. It will be interesting to see if *H. naledi*, a small-brained hominin, is like other small-brained hominins in developing its dentition more rapidly than modern humans (Bromage and Dean, 1985; Beynon and Wood, 1987; Beynon and Dean, 1991; Dean et al., 2001; Smith et al., 2015) or at the rapid end of the modern human spectrum (Dean and Liversidge, 2015). The large dental sample of *H. naledi*, which includes both deciduous and permanent teeth, will provide

an unparalleled opportunity to understand patterns and rates of dental growth and development in an extinct hominin species.

Acknowledgments

A Wenner-Gren grant awarded to L.K.D. and M.M.S. funded D.G.S.'s and A.L.C.'s attendance at a *Homo naledi* dental workshop at the University of the Witwatersrand in July, 2016. Support for L.K.D. was also provided by a Connor Family Faculty Fellowship and by the Office of Research and Development at the University of Arkansas.

At the University of Witwatersrand, Bernard Zipfel provided access and help with the fossil specimens. We thank Darryl de Ruiter for supporting this project and Mark Skinner for helping with casting these teeth as well as for fruitful discussions. We thank Christopher Dean for sharing data. We thank Emma Lagan for help with the images of *Homo naledi* teeth. Light optical images for perikymata counting were acquired using a Leica DMS 1000 digital monocular microscope at the Subsurface Energy Materials Characterization and Analysis Laboratory (SEMCAL), School of Earth Sciences, The Ohio State University with the help of Julie Sheets. The measuring microscope used in this study was supported by NSF grant BCS-0607520 to D.G.S. This work is also supported by NSF Foundation Graduate Research Fellowship Program Grant No. DGE-1343012 to M.C.O. Finally, we thank the Editor (David Alba), Associate Editor (Clément Zanolli), and three anonymous reviewers for their thoughtful comments that helped strengthen this paper.

Supplementary Online Material

Supplementary online material related to this article can be found at <https://doi.org/10.1016/j.jhevol.2018.03.007>.

References

- Ahern, J.C., Hawks, J.D., Lee, S.H., 2005. Neandertal taxonomy reconsidered... again: a response to Harvati et al. (2004). *Journal of Human Evolution* 48, 647–652.
- Arsuaga, J., Martínez, I., Arnold, L., Aranburu, A., Gracia-Téllez, A., Sharp, W.D., Quam, R.M., Falguères, C., Pantoja-Pérez, A., Bischoff, J., Poza-Rey, E., Parés, J.M., Carretero, J.M.M., Demuro, M., Lorenzo, C., Sala, M., Martínón-Torres, M., García, N., Alcázar de Velasco, A.G., Cuenca-Bescós, G., Gómez-Olivencia, A., Moreno, D., Pablos, A., Shen, C.-C., Rodríguez, L., Ortega, A.I., García, R., Bonmatí, A., Bermúdez de Castro, J.M., Carbonell, E., 2014. Neandertal roots: cranial and chronological evidence from Sima de los Huesos. *Science* 344, 1358–1363.
- Berger, L.R., Hawks, J., de Ruiter, D.J., Churchill, S.E., Schmid, P., Deleuzene, L., Kivell, T.L., Garvin, H.M., Williams, S.A., DeSilva, J.M., Skinner, M.M., Musiba, C.M., Cameron, N., Holliday, T.W., Harcourt-Smith, W., Ackerman, R.R., Bastir, M., Bogin, B., Bolter, D., Brophy, J., Cofran, Z.D., Congdon, K.A., Deane, A.S., Dembo, M., Drapeau, M., Elliot, M.C., Feuerriegel, E.M., Garcia-Martinez, D., Green, D.J., Gurtov, A., Irish, J.D., Kruger, A., Laird, M.F., Marchi, D., Meyer, M.R., Nalla, S., Negash, E.W., Orr, C.M., Radovic, D., Schroeder, L., Scott, J.E., Throckmorton, Z., Tocheri, M.S., VanSickle, C., Walker, C.S., Wei, P., Zipfel, B., 2015. *Homo naledi*, a new species of the genus *Homo* from the Dinaledi Chamber, South Africa. *eLife* 4, e09560.
- Berthaume M.A., Deleuzene L.K. and Kupczik K., Ecological differentiation in *Homo naledi*, *Journal of Human Evolution*, (in press).
- Beynon, A., Dean, M., 1991. Hominid dental development. *Nature* 351, 196.
- Beynon, A., Wood, B., 1987. Patterns and rates of enamel growth in the molar teeth of early hominids. *Nature* 326, 493–496.
- Bromage, T.G., Dean, M.C., 1985. Re-evaluation of the age at death of immature fossil hominids. *Nature* 317, 525–527.
- Dean, M.C., 1987. Growth layers and incremental markings in hard tissues: a review of the literature and some preliminary observations about enamel structure in *Paranthropus boisei*. *Journal of Human Evolution* 16, 157–172.
- Dean, M.C., 2009. Extension rates and growth in tooth height of modern humans and fossil hominin canines and molars. In: Koppe, T., Meyer, G., Alt, K.W. (Eds.), *Comparative Dental Morphology*. Karger, Basel, pp. 68–73.
- Dean, M.C., Beynon, A.D., Reid, D.J., Whittaker, D.K., 1993. A longitudinal study of tooth growth in a single individual based on long- and short-period incremental markings in dentine and enamel. *International Journal of Osteoarchaeology* 3, 249–264.
- Dean, C., Leakey, M.G., Reid, D., Schrenk, F., Schwartz, G.T., Stringer, C., Walker, A., 2001. Growth processes in teeth distinguish modern humans from *Homo erectus* and earlier hominins. *Nature* 414, 628–631.
- Dean, M., Reid, D., 2001a. Perikymata spacing and distribution on hominid anterior teeth. *American Journal of Physical Anthropology* 116, 209–215.
- Dean, M., Reid, D., 2001b. Anterior tooth formation in *Australopithecus* and *Paranthropus*. In: Brook, A. (Ed.), *Dental Morphology*. Sheffield Academic Press, Sheffield, pp. 135–149.
- Dean, M.C., Liversidge, H.M., 2015. Age estimation in fossil hominins: comparing dental development in early *Homo* with modern humans. *Annals of Human Biology* 42, 413–427.
- Dean, M.C., Shellis, R.P., 1998. Observations on stria morphology in the lateral enamel of *Pongo*, *Hylobates*, and *Proconsul* teeth. *Journal of Human Evolution* 35, 401–410.
- Deleuzene, L.K., Brophy, J.K., Skinner, M.M., Gurtov, A.N., Hawks, J., Irish, J.D., Berger, L.R., de Ruiter, D.J., 2016. Metric and nonmetric features of the *Homo naledi* dentition. *American Journal of Physical Anthropology* 162, 128–129.
- Dembo, M., Radović, D., Garvin, H.M., Laird, M.F., Schroeder, L., Scott, J.E., Brophy, J., Ackermann, R.R., Musiba, C.M., de Ruiter, D.J., Moors, A., Collard, M., 2016. The evolutionary relationships and age of *Homo naledi*: an assessment using dated Bayesian phylogenetic methods. *Journal of Human Evolution* 97, 17–26.
- Dirks, P.H.G.M., Roberts, E.M., Hilbert-Wolf, H., Kramers, J.D., Hawks, J., Dosseto, A., Duval, M., Elliot, M., Evans, M., Grün, R., Hellstrom, J., Herries, A.I.R., Joannes-Boyau, R., Makhubela, T.V., Placzek, C.J., Robbins, J., Spandler, C., Wiersma, J., Woodhead, J., Berger, L., 2017. The age of *Homo naledi* and associated sediments in the Rising Star Cave, South Africa. *eLife* 6, e24231.
- FitzGerald, C.M., 1998. Do enamel microstructures have regular time dependency? Conclusions from the literature and a large-scale study. *Journal of Human Evolution* 35, 371–386.
- Garvin, H., Elliott, M., Deleuzene, L.K., Hawks, J., Churchill, S., Berger, L., Holliday, T., 2017. Body size, brain size, and sexual dimorphism in *Homo naledi*. *Journal of Human Evolution* 11, 119–138.
- Guatelli-Steinberg, D., Floyd, B.A., Dean, M.C., Reid, D.J., 2012. Enamel extension rate patterns in modern human teeth: two approaches designed to establish an integrated comparative context for fossil primates. *Journal of Human Evolution* 63, 475–486.
- Guatelli-Steinberg, D., O'Hara, M., Xing, S., Reid, D.J., 2016. Perikymata distribution relative to total perikymata number within the genus *Homo*. *American Journal of Physical Anthropology* 159, 562, 163.
- Guatelli-Steinberg, D., Reid, D.J., Bishop, T.A., 2007. Did the lateral enamel of Neandertal anterior teeth grow differently from that of modern humans? *Journal of Human Evolution* 52, 72–84.
- Guatelli-Steinberg, D., Reid, D.J., Bishop, T.A., Larsen, C.S., 2005. Anterior tooth growth periods in Neandertals were comparable to those of modern humans. *Proceedings of the National Academy of Sciences USA* 102, 14197–14202.
- Harvati, K., Frost, S.R., McNulty, K.P., 2004. Neandertal taxonomy reconsidered: implications of 3D primate models of intra- and interspecific differences. *Proceedings of the National Academy of Sciences USA* 101, 1147–1152.
- Hawks, J., Elliott, M., Schmid, P., Churchill, S.E., Ruiter, D.J., de Roberts, E.M., Hilbert-Wolf, H., Garvin, H.M., Williams, S.A., Deleuzene, L.K., Feuerriegel, E.M., Randolph-Quinney, P., Kivell, T.L., Laird, M.F., Tawane, G., DeSilva, J.M., Bailey, S.E., Brophy, J.K., Meyer, M.R., Skinner, M.M., Tocheri, M.W., VanSickle, C., Walker, C.S., Campbell, T.L., Kuhn, B., Kruger, A., Tucker, S., Gurtov, A., Hlophe, N., Hunter, R., Morris, H., Peixotto, B., Ramalepa, M., Rooyen, D. van, Tsikoane, M., Boshoff, P., Dirks, P.H., Berger, L.R., 2017. New fossil remains of *Homo naledi* from the Lesedi Chamber, South Africa. *eLife* 6, e24232.
- Hillson, S., 2014. *Tooth Development in Human Evolution and Bioarchaeology*. Cambridge University Press, Cambridge.
- Hillson, S., Bond, S., 1997. Relationship of enamel hypoplasia to the pattern of tooth crown growth: a discussion. *American Journal of Physical Anthropology* 104, 89–103.
- Huda, T.F., Bowman, J.E., 1994. Variation in cross-striation number between striae in an archaeological population. *International Journal of Osteoarchaeology* 4, 49–52.
- Kawasaki, K., Tanaka, S., Ishikawa, T., 1977. On the incremental lines in human dentine as revealed by tetracycline labeling. *Journal of Anatomy* 123, 427–436.
- Le Cabec, A., Tang, N.K., Tafforeau, P., 2015. Accessing developmental information of fossil hominin teeth using new synchrotron microtomography-based visualization techniques of dental surfaces and interfaces. *PLoS One* 10, e0123019.
- Modesto-Mata, M., Dean, C., Gracia, A., Martínón-Torres, M., Martín-Francés, L., Guatelli-Steinberg, D., Reid, D., Martínez, I., Arsuaga, J.L., Bermúdez de Castro, J.M., 2014. Estudio comparado de los perikymata en los dientes del homínido XVIII de la Sima de los Huesos (Sierra de Atapuerca)/Comparative study of perikymata in the teeth of hominin XVIII from Sima de los Huesos (Sierra de Atapuerca). In: Alonso, S., Hervella, M., Izagirre, N., Peña, J.A., Rebato, E., de la Rúa, C. (Eds.), *La Investigación en Antropología Física: Una Mirada al Futuro*. Universidad del País Vasco, Bilbao, pp. 467–480.
- Modesto-Mata, M., García-Campos, C., Martín-Francés, L., Martínez de Pinillos, M., García-González, R., Quintino, Y., Canals, A., Lozano, M., Dean, M.C., Martínón-Torres, M., Bermúdez de Castro, J.M., 2017. New methodology to reconstruct in 2-D the cuspal enamel of modern human lower molars. *American Journal of Physical Anthropology* 163, 824–834.
- Ramirez-Rozzi, E.V., Bermúdez de Castro, J.M., 2004. Surprisingly rapid growth in Neandertals. *Nature* 428, 936–939.
- Randolph-Quinney, P.S., 2015. The mournful ape: conflating expression and meaning in the mortuary behaviour of *Homo naledi*. *South African Journal of Science* 111, #a0131.
- Rasband, W.S., 2016. ImageJ. U. S. National Institutes of Health, Bethesda, Maryland, USA. <https://imagej.nih.gov/ij/>.
- Reich, D., Green, R.E., Kircher, M., Krause, J., Patterson, N., Durand, E.Y., Viola, B., Briggs, A.W., Stenzel, U., Johnson, P.L.F., Maricic, T., Good, J.M., Marques-Bonet, T., Alkan, C., Fu, Q., Mallick, S., Li, H., Meyer, M., Eichler, E.E., Stoneking, M., Richards, M., Talamo, S., Shunkov, M.V., Derevianko, A.P., Hublin, J.J., Kelso, J., Slatkin, M., Pääbo, S., 2010. Genetic history of an archaic hominin group from Denisova Cave in Siberia. *Nature* 468, 1053–1060.
- Reid, D.J., Dean, M.C., 2006. Variation in modern human enamel formation times. *Journal of Human Evolution* 50, 329–346.

- Reid, D.J., Ferrell, R.J., 2006. The relationship between number of striae of Retzius and their periodicity in imbricational enamel formation. *Journal of Human Evolution* 50, 195–202.
- Saunders, S.R., Chan, A.H., Kahlon, B., Kluge, H.F., FitzGerald, C.M., 2007. Sexual dimorphism of the dental tissues in human permanent mandibular canines and third premolars. *American Journal of Physical Anthropology* 133, 735–740.
- SAS Institute Inc, 2008. SAS/STAT 9.2. User's Guide. SAS Institute Inc., Cary.
- Shellis, R., 1984. Variations in growth of the enamel crown in human teeth and a possible relationship between growth and enamel structure. *Archives of Oral Biology* 29, 697–705.
- Smith, B.H., 1984. Patterns of molar wear in hunter–gatherers and agriculturalists. *American Journal of Physical Anthropology* 63, 39–56.
- Smith, T.M., Tafforeau, P., Le Cabec, A., Bonnin, A., Houssaye, A., Pouech, J., Moggi-Cecchi, J., Manthi, F., Ward, C., Makaremi, M., Menter, C.G., 2015. Dental ontogeny in Pliocene and Early Pleistocene hominins. *PLoS One* 10, e0118118.
- Thackeray, F.J., 2015. Estimating the age and affinities of *Homo naledi*. *South African Journal of Science* 111. #a0124.
- Xing, S., Guatelli-Steinberg, D., O'Hara, M., Wu, X., Liu, W., Reid, D.J., 2015. Perikymata distribution in *Homo* with special reference to the Xujia Yao juvenile. *American Journal of Physical Anthropology* 157, 684–693.